SOLID MATTER

J.F.R. ARCHILLA,[1] Y.A. KOSEVICH,[2] N. JIMÉNEZ,[3] V.J. SÁNCHEZ-MORCILLO,[3] L.M. GARCÍA-RAFFI[4]

[1] Grupo de Física No Lineal. Universidad de Sevilla. Departamento de Física,
  Aplicada I. ETSI Informática,
  (Avda. Reina Mercedes, s/n. 41012-Sevilla, Spain; e-mail: archilla@us.es)
[2] Semenov Institute of Chemical Physics, Russian Academy of Sciences
  (Ul. Kosygina 4, 119991 Moscow, Russia)
[3] Instituto de Investigación para la Gestión, Integrada de las Zonas Costeras,
  Universidad Politécnica de Valencia,
  (C/.Paranimfo 1, 46730 Grao de Gandia, Spain)
[4] Instituto de Universitario Matemática Pura y Aplicada, Universidad Politécnica de Valencia
  (Camino de Vera s/n, 46022 Valencia, Spain)

MOVING EXCITATIONS IN CATION LATTICES

We consider a model made out of identical particles that repel each other with the Coulomb interaction. We study numerically and analytically the existence and properties of supersonic kinks, showing that they are very easy to be produced and propagate long distances. They have a wide range of velocities and energies. We are motivated by a special characteristic of the muscovite mica mineral. Tracks from particles such as muons can be distinguished in a complex decoration, but the only explanation to most of the tracks is localized excitations called quodons. They move in the cation lattice, sandwiched between the silicate layers, along the lattice directions. Quodons have also been observed experimentally [EPL 78 (2007) 1005].

K e y w o r d s: excitations, quodons, cation lattices, Coulomb interaction.

1. Introduction

Charged particles are known to produce tracks in solids in what now is a well-established discipline called solid-state nuclear tracks detectors (SSNTDs). Usually, the first finding is attributed to Young in 1958 [1] in a lithium fluoride crystal, followed very closely by Silk and Barnes in 1959 [2], who found tracks from fission fragments in natural mica. Later, Price and Walker in 1962 reported on the observation of fossil particle tracks also in natural mica [3].

In natural minerals, tracks are a record of phenomena occurring in geological times during millions of years and in inaccessible places like the interior of the Earth or the outer space, both because the mineral is found inside meteorites [4]. Minerals can also integrate events for extremely long times far beyond the laboratory possibilities, by recording, therefore, very rare or infrequent events. They show different responses to different particles, filtering out the background of particles that would blur the tracks of particles or energies of interest.

They have been used, for example, to find the exotic spontaneous emission of ^{14}C clusters by ^{223}Rn [5] or to find the long tracks produced by the natural decay of superheavy elements ($Z > 110$) already disappeared [6]. Natural minerals are also useful for the fission track dating, oil search, and many other applications. See Refs. [7, 8] for reviews. Tracks are produced very often only under some specific conditions of the temperature and the pressure of a cool-

ing process during the mineral formation in the so-called sensitive period. The tracks become fossilized thereafter.

Muscovite mica is a layered silicate, which can be split in thin films due to its layered structure. The layers are composed of a layer of silicate octahedra between two layers of silicate tetrahedra sharing oxygen atoms. About one of four tetrahedral Si^{4+} is replaced by Al^{+3} leading to a net negative charge, which is compensated by a layer of K^+ cations joined feebly the silicate sheets [9]. The height of the silicate layers is about 7 Å, and that of an interlayer is 3.36 Å, where the K^+ ions are sitting. The K^+ ions form a two-dimensional lattice, which is approximately hexagonal with close packed lines at angles very close to 60°. The muscovite structure can be seen at the top of Fig. 1 and the interlayer lattice at the bottom.

Very thin sheets of muscovite can be easily separated down to a thickness of, theoretically, a few Å. About a half of the K^+ ions remains attached to each layer, but the silicate structure remains intact. This gives a possibility of inspecting the interior of a mineral without actually breaking it. Many specimens of muscovite show dark lines, made out of iron oxide, Fe being a common impurity in muscovite. Most of the lines are parallel to one another along the three main directions of the 2D lattice, but about 1% are at random directions, which means that they are not related to the lattice structure.

The close inspection of the random lines reveals that they are not exactly straight but show many small kinks, like a charged particle interacting with nuclei of a crystal. The measurements of the lengths and the kink angles of the minority lines were consistent with the Coulomb scattering of muons produced by neutrinos in cosmic rays, which can penetrate into a deep underground [10]. The evidence of electron showers caused by muons [11] and positrons emitted by the decay of ^{40}K [12–14] was also found. The recording process was described as the precipitation of iron oxide that would grow by accretion.

The research described above showed that mica has an amazing capability of recording the disturbances produced by charged particles over a wide range of energies, but this leaves the majority of the lines oriented along the close packed lines of the 2D cation lattice to be unexplained. Those lines are straight, suggesting that they are not produced by a particle
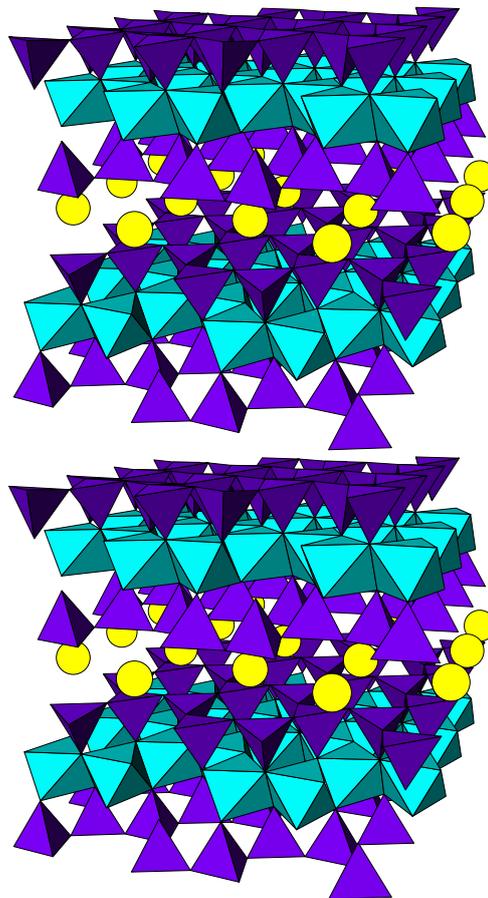

Fig. 1. Crystal structure of muscovite. The circles represent the potassium ions forming the interlayer sheet. The unit cell includes two silicate layers and two K^+ ions with parameters $a = 5.19$ Å; $b = 9.02$ Å; $c = 20.0$ Å; and $\beta = 95.7°$

scattered by nuclei. More likely, such lines have to be produced as some kind of an anharmonic excitation traveling along the lattice without dispersion [15, 16] in the form of a nonlinear quasi-one-dimensional excitation or *quodon*, a name originally proposed in [17].

The experimental confirmation of the existence of quodons was obtained by launching an alpha particle against a mica specimen and detecting the ejection of an atom a few millimeters apart at the opposite boundary, at angles corresponding to the lattice main directions [18].

The particular fast kinetics of the reconstructive transformation of muscovite has been related to the existence of transversal *breathers* or localized nonlinear vibrations [19–21]. However, they are not good
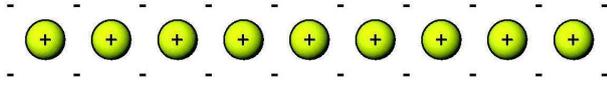
Fig. 2. Sketch of Coulomb's chain. The yellow spheres represent K$^+$ ions surrounded by the negative charge of the silicate layers above and below

candidates for quodons, as they move slowly, radiate, and have energies of only a few eV.

The cation lattice presents an important characteristic, which, in our opinion, has not been taken into account, even being quite evident: cations experience repulsive interactions which decay with the distance, generating a *repulsive lattice*. The interaction is mainly of the Coulomb type, but also there exist repulsive short-range forces at shorter distances. There are also the van der Waals forces, but they are smaller in magnitude with respect to the other forces. There is also the interaction with the other atoms in the silicate layers which produces a periodic potential. To make it clear, let us enumerate what repulsive lattices do not have, though it is usually used in a modeling: a) They do not have an equilibrium distance, as the Lennard-Jones, Morse, or Toda potentials have, as they are always repulsive; b) The pair potential does not increase with the relative distance, as this happens in α- and β-FPU lattices, which are the first terms of a Taylor series and, consequently, are strictly valid only for relatively small amplitude vibrations.

As the first step to study the implication of our hypothesis, we construct a minimal model, where we keep only explicitly the Coulomb interaction between the cation atoms, although other contributions will be taken implicitly, as explained below.

We observe that supersonic kinks [22] with as much energy as desired can propagate long distances unaffected by phonons and rebounding with others.

2. Model

We construct a minimal model of K$^+$ in the cation layer in order to observe the properties of a repulsive lattice. It will be augmented in future works. Our hypotheses are: (a) We assume the system is one-dimensional and oriented along a close packed line with unit distance $a = 5.19$ Å. Moreover, the movement of particles is longitudinal and limited to the same direction. (b) The electric field and other interactions with the silicate layers are not taken into ac-

count explicitly, but they are implicitly, as they bring about the actual lattice unit a in equilibrium. (c) We consider here, for simplicity, only the nearest neighbor Coulomb interaction (the effect of more neighbors is shortly discussed later). (d) The effect of the interaction with the silicate layers is also taken into account as something fixing the particles in place at a distance a in equilibrium. Figure 2 shows a sketch of the model.

The justification of (b) is that the neutrality of the crystal by itself will produce a two-dimensional lattice with the actual positive charge density so as to compensate the negative charge in the silicate layers. Then, it also determines the interatomic spacing within a close packed hexagonal structure.

The equation of motion of a K$^+$ ion is given by

$$m\ddot{x}_n = -\frac{\mathrm{K_C}e^2}{(x_{n+1} - x_n)^2} + \frac{\mathrm{K_C}e^2}{(x_n - x_{n-1})^2}. \qquad (1)$$

We can write the equation in dimensionless form by choosing $a = 5.19$ Å, $\tau = \sqrt{m_\mathrm{K}a^3/\mathrm{K_C}e^3} = 0.1989$ ps $\simeq 0.2$ ps, and $m_{\mathrm{K}+} = 39.1$ amu as the units of distance, time, and mass, respectively. We define the displacement with respect to the equilibrium position u_n, measured in lattice units as $x_n = an + au_n$. The dimensionless units of other magnitudes correspond to the following approximate values: velocity 2.6 km/s; energy 2.8 eV, and frequency 5 THz.

The dimensionless dynamic equations become:

$$\ddot{u}_n = -\frac{1}{(1 + u_{n+1} - u_n)^2} + \frac{1}{(1 + u_n - u_{n-1})^2}. \qquad (2)$$

There are two fixed particles at the borders so as the system is confined between its boundaries. However, we do not pretend to model a realistic border, as we are interested in what is happening far away from it, which does not depend on the specific boundary conditions.

3. Phonons

For small amplitudes, Eq. (2) reduces to

$$\ddot{u}_n = \mathrm{c}^2(u_{n+1} + u_{n-1} - 2u_n), \qquad (3)$$

where $\mathrm{c} = \sqrt{2}$ with our scaling is the speed of sound.

The dispersion relation and velocities are well known; we include them here for comparison with

what follows later. The phonon frequencies are

$$\omega_{\mathrm{ph}} = \omega_{\mathrm{M}} \sin(q/2),$$

$$q = \frac{2\pi m}{N}, \; m = 0, 1, ..., N-1, \tag{4}$$

with $\omega_{\mathrm{M}} = 2c$ being the maximum frequency, corresponding to the mode with the wave number $q = \pi$. The phase velocity $V_{\mathrm{ph}} = \omega/q$ and the group velocity $V_{\mathrm{g}} = \partial\omega/\partial q$ are given by

$$V_{\mathrm{ph}} = c\frac{\sin(q/2)}{q/2}, \quad V_{\mathrm{g,ph}} = c\cos(q/2). \tag{5}$$

In the limit of long wavelengths, both velocities are equal to the speed of sound c, which is also the maximum value. Note that the group velocity becomes zero at the top of the phonon band $q = \pi$.

The maximum frequency in physical units is about 2.2 THz, which is larger than that obtained with molecular dynamics and neutron spectroscopy to be about 1.6 THz [24–26]. This is understandable due to the simplicity of our model considering just one type of atoms compared with the complexity of real mica, but it is within the same range of values. Figure 3 shows the phase and group velocities in physical units. Note that the predicted speed of sound is similar to that found in Ref. [23] to be 3.4–3.7 km/s.

Note that, for phonons, we have taken periodic boundary conditions, as we are interested in traveling waves far from the borders of the system.

4. Tails

4.1. Tail analysis

We are interested in traveling nonlinear localized solutions supported by the Coulomb lattice. Although they correspond to the full nonlinear equation, their tails have small amplitude and can be studied with the linear equation above. Note that the tails do not exist by themselves, but they give useful information about the kinks, solitons, or breathers, to which they belong. Figure 4 shows a soliton with front and back tails.

As it is standard, we propose the following tail solution:

$$u_n = \exp(-\xi(n - Vt))\exp(i(qn - \omega t)). \tag{6}$$

Supposing that the tail is moving to the right with velocity $V > 0$, the front tail correspond to $\xi > 0$, and
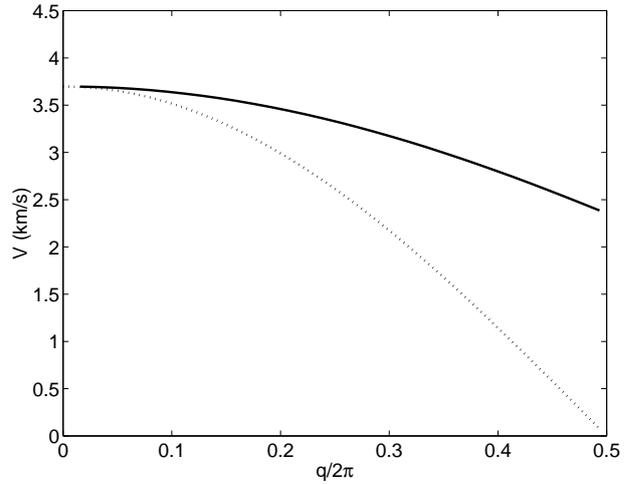

Fig. 3. Phase (continuous line) and group (dotted) velocities in Coulomb's chain as a function of the wave number. In the limit of long wavelengths, both give the sound velocity, which can be compared with the values of 3.4–3.7 km/s obtained in Ref. [23]
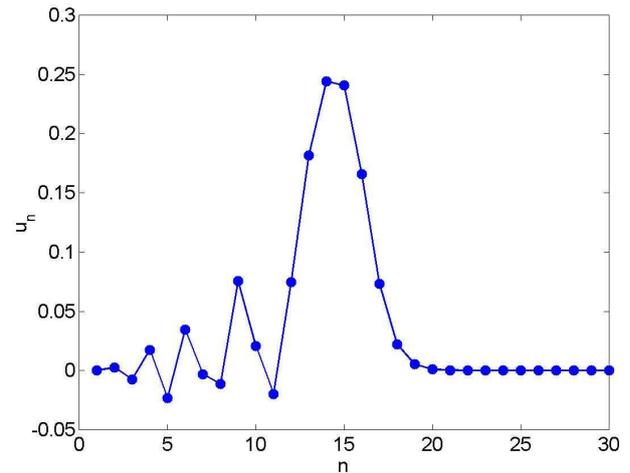
Fig. 4. Profile of the transitory state of a soliton with low amplitude moving to the right showing the front and back tails. The subsonic oscillatory back tail will be left behind the supersonic soliton. The front tail becomes so steep that, in practice, it becomes the abrupt end of a perturbation. Therefore, the soliton will transform to a kink, and the back tail without the support of the soliton will be dispersed in phonons. Dimensionless units

it is also valid ahead of the center of the excitation, i.e., for $n > Vt$. The back tail corresponds to $\xi < 0$, and it needs that $n < Vt$. The modulus of ξ is the localization parameter, and its inverse $\Lambda = 1/|\xi|$ is
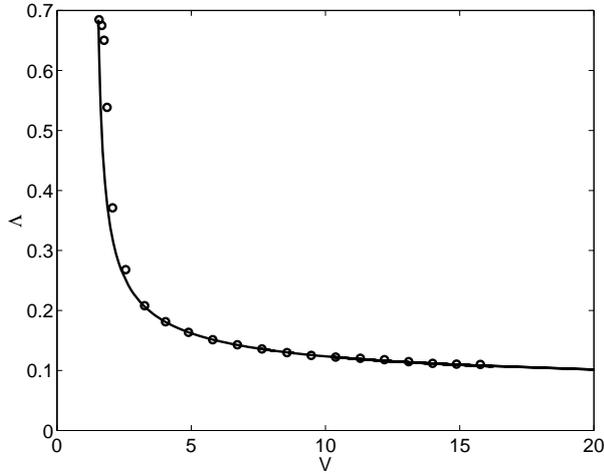
Fig. 5. Comparison of the numerical (circles) and theoretical (continuous line) decay lengths as a function of the velocity for a kink with magic wave number (see text). Dimensionless units

the decay length. We recover the phonons for the limit of zero localization, that is $\xi = 0$.

The substitution in Eq. (3) allow us to obtain the frequency and the velocity of the tails as a function of the wave number and the localization parameter. The tail frequency ω is given by

$$\omega = \cosh(\xi/2)\,\omega_{\mathrm{ph}} = \cosh(\xi/2)\,\omega_{\mathrm{M}}\sin(q/2), \qquad (7)$$

with ω_{ph} being the phonon frequency given in Eq. (4).

The velocity of the tail is given by

$$V = \frac{\sinh(\xi/2)}{\xi/2}\,V_{\mathrm{g,ph}} = \frac{\sinh(\xi/2)}{\xi/2}\,c\,\cos(q/2), \qquad (8)$$

$V_{\mathrm{g,ph}}$ being the phonon group velocity given in Eq. (5). These equations were first obtained by one of the authors [27] for the analysis of discrete solitons.

As $\sinh(\xi/2)/(\xi/2)$ and $\cosh(\xi/2)$ are both larger than unity and monotonically increasing functions of $|\xi|$, we conclude that the tails oscillate and move faster than the phonons.

The relationship between the decay length $\Lambda = 1/|\xi|$ and V given by the equation above is in excellent agreement with the numerical results, as can be seen in Fig. 5.

4.2. Breathers

If $\omega \neq 0$, the tails are oscillating and may correspond to breathers, localized oscillating solutions with a frequency above the phonon band. The conditions for

the existence of breathers in FPU systems can be analyzed [15, 28] in terms of the derivatives of the pair potential $V(y)$. If $V'(0) = 0$, $V''(0) = 1$ and $V^{(4)}(0)/2 < |V^{(3)}(0)|^2 < 2V^{(4)}(0)$, there are no small amplitude breathers, but there are large amplitude breathers (LAB).

Small amplitude breathers are those that can be continued down to the phonon band, while there are the energy and amplitude gaps for large amplitude breathers.

The above condition cannot be directly applied to the Coulomb potential, as it has no local minimum. However, we can consider another pair potential $W(y) = 1/|1 + y| + y$, defined for $y > -1$, with a derivative $W'(y) = 1 - 1/(1 + y)^2$ which is zero at $y = 0$. For the total potential $W_T = \sum_n W(u_n - u_{n-1})$, we obtain that $\ddot{u}_n = -W'(u_n - u_{n-1}) + W'(u_{n+1} - u_n) = -V'(u_n - u_{n-1}) + V'(u_{n+1} - u_n)$, as the constant terms in the derivatives cancel out. The derivatives of W are $W^{(\mathrm{n})}(0) = V^{(\mathrm{n})}(0) = (-1)^n n!$, for $n > 1$, and it is easy to check that the condition for the existence of LABs holds.

Therefore, large amplitude breathers should exist in our system, but to find them numerically is not trivial. The continuation from an artificial solution has to be done during a long path, where annihilation bifurcations are encountered. We have not been able to find them, and it is also possible that the theorems on the LAB existence do not hold in our system due to the slow convergence of the Taylor series for the Coulomb potential. In addition, it may be due to the fact that W is a mathematical trick, as there is no real minimum of V at $y = 0$. We can construct similar potentials $1/r + \alpha r$ with minima at any distance. The subject is interesting enough, and we continue doing the research on it, but breathers are not the main interest of this article, centered in moving kinks.

4.3. Oscillating tails

The frequency and the velocity given by Eqs. (7) and (8) may correspond not only to a breather but also to the front or back tails of a soliton or a kink. We can see that both the frequency and the velocity increase with the localization $|\xi|$, but they depend on the wave number q in opposite ways, as the frequency is maximum for $q = \pi$, when the velocity is zero, and the velocity is maximum for $q = 0$ and zero for $q = \pi$.

If the frequency of the tails is inside the phonon band, the tails become unstable, the mode $q = \pi$ would be the most stable, as its frequency is always larger than ω_M, but its velocity is zero. On the other hand, large values of $|\xi|$ are unrealistic because, in practice, they mean a steep end of the nonlinear excitation. So, there is the need to balance the effects of the wave number and the localization.

A particular value of the wave number, with interesting properties, is $q = 2\pi/3$, the so-called *magic number* [22]. It allows analytical estimations, as will be explained below. The frequency and the velocity become

$$\omega = \sqrt{3}c\cosh(\xi/2); \quad V = \frac{c\sinh(\xi/2)}{\xi}. \tag{9}$$

For the frequency of the tail to be above the phonon band, we need that $\xi > \xi_0 = 1.0986$. For $\xi = \xi_0$, each particle amplitude is exactly one third smaller than the previous one, and the velocity $V \approx c/3$, one third of the sound velocity. To attain the sound velocity, the localization has to be about $\xi = 6.5$, but this value corresponds to a change in the amplitude of three orders of magnitude in the particle amplitude, which describes an abrupt end of the soliton or kink and not an actual tail.

This is the procedure to produce a supersonic kink, the subsonic back tail is left behind, while the supersonic front tail is, in reality, a sudden beginning of a kink.

4.4. Tails of solitons and kinks

Solitons are localized, traveling non-oscillatory excitations, that is, with $V \neq 0$ and $\omega = 0$. From Eq. (7), it follows that $\sin(q/2) = 0$ or $q = 0$ (solitons are in-phase modes). Substituting into Eq. (8), we obtain the soliton velocity as a function of the localization ξ:

$$V_{\rm sol} = \frac{\sinh(\xi/2)}{\xi/2}\, c. \tag{10}$$

Two important conclusions arise: a) Solitons do not have an internal structure, as they come from the mode $q = 0$, all the atoms are in-phase, and the minimum value of the velocity of a soliton is c, the sound velocity, which is also the maximum phonon velocity. Therefore, the solitons, differently from oscillating tails, are supersonic.

As commented above, it is possible to have different tail solutions for the front and the back. For example, in principle, it is possible to have a front soliton followed by a simple translation $x_n = a$, which would be a kink that leaves behind the atoms displaced one lattice unit, or the back tail may be an oscillatory tail, traveling at a subsonic speed, being left behind by the supersonic soliton at the front, as shown in Fig. 4. The front tail needs to be so steep to move in front of the soliton, which means in practice that the front of the soliton finishes abruptly, and the soliton becomes a kink. Of course, if these properties hold, the study of the full system with full potentials is required, which will be done in the next sections, but it is also essential to know the behavior of the system at low amplitudes, because a part of the system corresponds to the description, when there is a localized nonlinear solution.

5. Kinks with Magic Wave Number

The previous subsections refer to the tail analysis, which actually is the same for any system, whose linear equation is Eq. (3). We can obtain much more information about the nonlinear excitation of the full system using the Rotating Wave Approximation (RWA) [29]. It consists in performing a Fourier transformation of the dynamical equations and approximating it to the first harmonic.

It is convenient to define a new variable, the relative displacement or strain of the chain, as $v_n = u_n - u_{n-1}$. From Eq. (2), we can easily obtain the evolution equation for the strain as

$$\ddot{v}_n = 2F_n - F_{n+1} - F_{n-1}; \quad \text{with} \quad F_n = \frac{1}{(1+v_n)^2}. \tag{11}$$

Kinks are characterized by a very steep profiles, with only a few particles moving at a given time. A solution presenting this behavior is given (in the strain representation) by a half-wavelength structure with the *magic* wave number $q = 2\pi/3$. Following Ref. [22], we propose the following ansatz describing a kink traveling to the right:

$$v_n = -\frac{A}{2}(1 + \cos(qn - \omega t)) \quad \text{if} \quad -\pi < qn - \omega t < \pi \tag{12}$$

and $v_n = 0$ otherwise. Equation (12) represents a solution, where 3 particles (the kink core) are in motion,
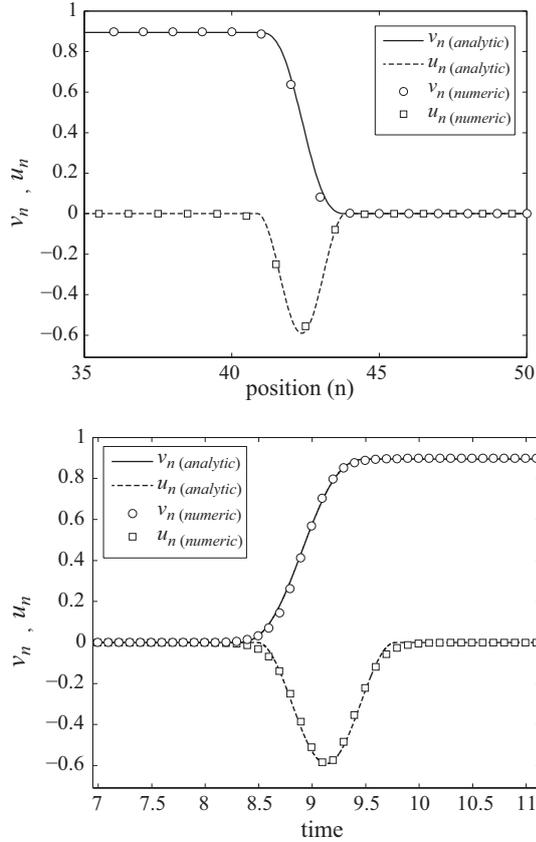
Fig. 6. Comparison between analytical and numerical results: (top) spatial profile of the kink traveling to the right. u_n are the coordinates of the particles relative to their initial displacements u_n, and $v_n = u_n - u_{n-1}$ are the strains. (Bottom) Evolution in time with a particle when reached by the kink
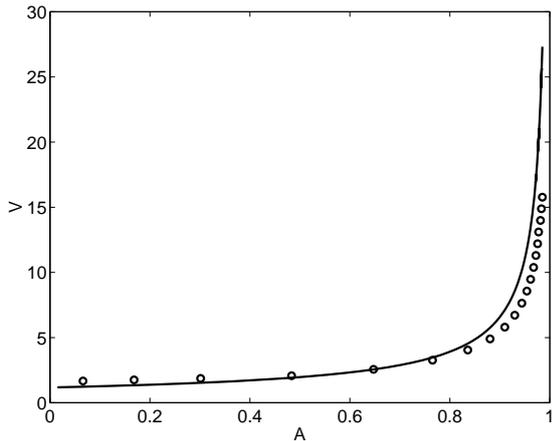
Fig. 7. Numerical (circles) and theoretical (continuous line) velocities of kinks within the RWA, for the magic wave number $q = 2\pi/3$. Dimensionless units

while the others remain at rest. Figure 6 shows the profiles and the temporal evolution of a kink given by this equation and compared with the numerical results.

When we substitute (12) in the equation of motion (11), the nonlinearity generates multiple frequencies. The RWA approximation states that the nonlinear contributions higher than the second harmonics can be neglected. This implies that the force terms can be approximated by their first-order Fourier expansions, as $F_n = a_0 + a_1 \cos(qn - \omega t)$. On the other hand, the left-hand side of Eq. (11) gives, after the substitution of Eq. (12), $\ddot{v}_n = (A/2)\omega^2 \cos(qn - \omega t)$ which is equal to the first harmonic term on the right-hand side. The zero harmonic cancels out due to the dependence of the right-hand side on F_n. The first harmonic of F_n is given by

$$a_1 = \frac{1}{\pi} \int\limits_{-\pi}^{\pi} \frac{\cos(\theta)\mathrm{d}\theta}{(1 - \frac{A}{2} - \frac{A}{2}\cos(\theta))^2} \,. \tag{13}$$

For $A < 1$, we obtain

$$a_1 = \frac{A}{(1 - A)^{3/2}}. \tag{14}$$

Therefore, substituting $\ddot{v}_n$ and $F_n = a_0 + a_1 \cos(qn - \omega t)$ in Eq. (11), we obtain the frequency and the velocity as functions of the amplitude A:

$$
\begin{aligned}
\omega &= \frac{1}{(1 - A)^{3/4}}\, \omega_{\mathrm{M}} \sin(q/2); \\
V &= \frac{\omega}{q} = \frac{1}{(1 - A)^{3/4}}\, c\frac{\sin(q/2)}{q/2}.
\end{aligned}
\tag{15}
$$

These magnitudes are equal to the corresponding ones for phonons, multiplied by a factor $1/(1 - A)^{3/4}$, which, of course, tends to 1, when A is small, but it diverges, when A approaches 1. The kink velocity as a function of the amplitude is shown in Fig. 7, where the quite good agreement with the numerical and theoretical results is observed. It is not so good when the amplitude approaches 1, when the RWA is less precise.

6. Numerical Simulations of Kinks

Kinks can be easily excited by sinusoidally perturbing the first particle of the lattice during half a period, so as it comes back to its initial position [22]. The amplitude A_0 and the frequency ω_0 of the initial perturbation are significant in the results, as they influence

the energy of a kink. In this way, we can create single kinks or, by increasing the initial amplitude, any number of kinks, as shown in Fig. 8. These kinks rebound at the borders and when they encounter each other, as it is the only physical possibility when two particles changing a position in different directions encounter each other. The evolution of two supersonic kinks is shown in Fig. 9.

The velocities of the kinks obtained numerically are very similar to the theoretical ones obtained within the RWA, as has been already presented in Fig. 7.

6.1. Kink profiles and energies

In Fig. 6, we show the kink profile, and the temporal evolution of the coordinates of a particle far enough from the borders. Both the displacements u_n with respect to the initial position and the relative displacements or strains $v_n = u_n - u_{n-1}$ are shown. The points represent the values obtained numerically, and the lines represent the values of v_n given by Eq. (12) for the magic wave number $q = 2\pi/3$. The theoretical values of u_n are obtained as $u_n(t) = \sum v_m(t)$. It can be seen that there is a very good agreement for both quantities.

The energies of kinks can be obtained easily, as the perturbed part of the lattice consists of almost only three particles, if we exclude the tails and the phonons that have been left behind. The kinetic energy is very close to $K = 1/2\,V^2$, which means that the kink behaves itself as a quasiparticle of unit mass (or a K^+ ion mass in physical units).

The energies of the kink in physical units are represented in Fig. 10 as a function of the kink velocity. The total energy E is constant, but the kinetic K and potential U energies change in time, so the values plotted are the maximum kinetic and potential energies, which are not attained at the same time. Because of that, the sum $K + U$ is different from E. As it can be seen, energies of hundred of eV are obtained. Increasing the frequency of the initial excitation, it is possible to obtain even keV. Of course, it is not known, if these energies can be obtained in real mica.

6.2. Evolution of the local energies

We can observe the evolution of the densities of kinetic, potential, and total energies for different kink amplitudes, considering a particle at a fixed site (e.g.,
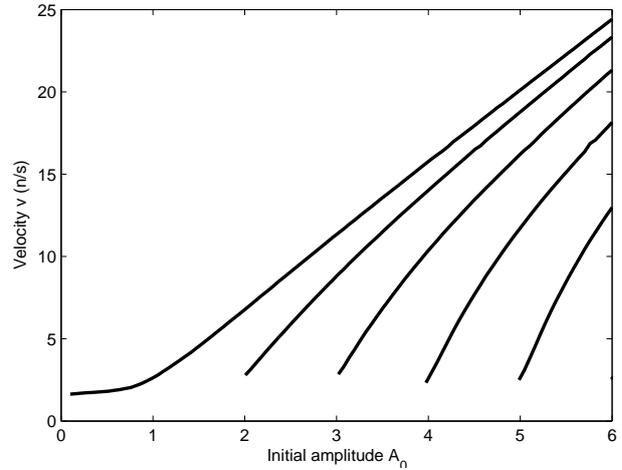

Fig. 8. Velocity and number of kinks as functions of the initial excitation amplitude A_0. Dimensionless units
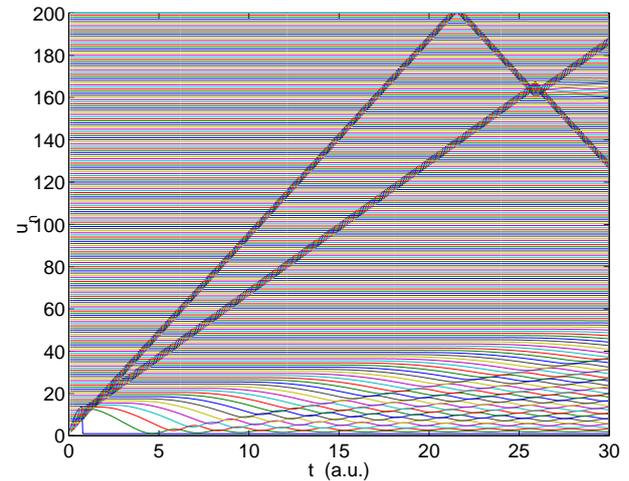

Fig. 9. Evolution of two kinks with more than four times the sound speed. Dimensionless units

$n = 30$) and the corresponding maximum values of the particle energy (kinetic, potential, and total ones), when the kink arrives to this position. In this case, the energy grows as soon as the amplitude of the kink approaches 1. The increase in the potential energy is in agreement with the repulsive character of the potential. The increase of the kinetic energy is also in agreement with the dependence of the velocity on the amplitude, as it is shown in Fig. 7 that has been obtained in the RWA approximation.

The behavior of the particle can be seen in more details in Fig. 11. When the kink arrives to the site
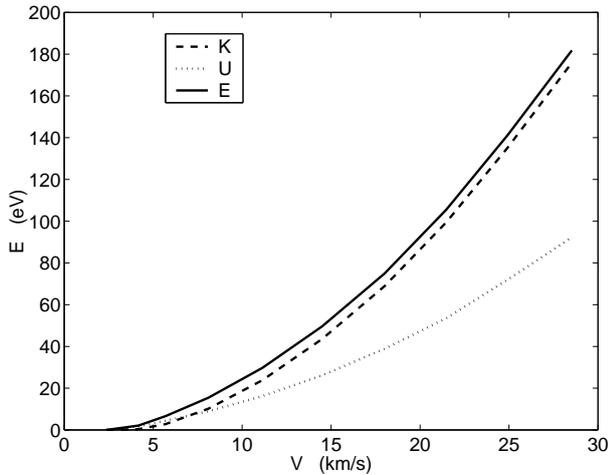
Fig. 10. Kink energies in physical units as a function of its velocity: the total energy E and the maximum kinetic K and potential U energies (see the text). The kinetic and total energies are very close to $\frac{1}{2}mV^2$ showing that the kink behaves itself as a quasiparticle
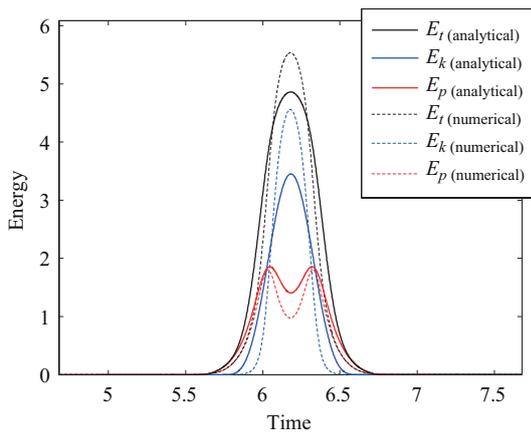
Fig. 11. Potential, kinetic, and total energies as functions of the amplitude for a fixed particle at site $n = 30$. The points are numerical values and the lines (dotted, dashed, and continuous ones for the potential, kinetic and total energies, respectively) represent the values deduced from the analytical solution for the relative displacements $v_n(t)$ from Eq. 12, and $u_n(t) = \sum v_n(t)$. The amplitude of the kink is $A = 0.78$

$n = 30$, the particle starts moving, returning, after some time, to the rest position. This situation is represented in this figure, by plotting the energies (potential, kinetic, and total ones) for the amplitude of the kink $A = 0.78$. It can be seen that the evolution of the local potential energy with time is a curve close
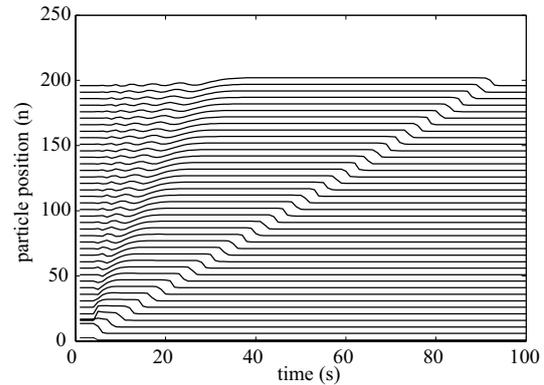
Fig. 12. Evolution of a supersonic kink in a lattice, where the Coulomb interaction with the nearest four neighbors has been taken into account. Dimensionless units

to a double Gaussian peak. This can be explained by the process of double pushing with the neighbors that suffers the particle. When the kink arrives to the site, the left-hand side neighbor of the particle pushes it to the right, increasing the displacement with high acceleration. But simultaneously, as the particle approaches the neighbor on the right-hand side, this neighbor pushes it just in the opposite direction, producing a deceleration as a result of the balance between these two forces, because the potential we have considered is repulsive. The valley at the center between the double peak becomes deeper as A reaches values closer to 1. For low values of the amplitude, peaks become wider, producing the unique wide peak flattened on top. The lines in Fig. 11 (dashed, dotted, and continuous ones) represent the values of these energies (potential, kinetic, and total ones) obtained from $u_n(t) = \sum v_n(t)$, where $v_n(t)$ is given by Eq. (12). The disagreement observed with the numerical values can be explained as a consequence of the limitation of the validity of $v_n(t)$ from Eq. (12) that has been obtained within the RWA.

6.3. Kinks with particles interacting between several neighbors

We have also checked that the kinks continue to exist if we extend the Coulomb interaction beyond nearest neighbors, although they become wider. Figure 12 shows the evolution of a kink, where we have considered the interaction with the first four neighbors. The localization and the supersonic speed of the kink are evident. However, the larger the number of neigh-

bors, the wider becomes the kinks. But we do not think that many neighbors should be taken because in the ions are not isolated a real crystal, and the rest of the crystal produces an screening effect.

Note that to consider a true long-range interaction with all neighbors is a completely different problem that we do not address here. As is known, this leads to a dependence of the sound speed on the number of particles as $N \log(N)$, which would be extremely large in a macroscopic crystal and diverges for $N \to \infty$. Solitons and kinks closer to the continuum limit have been studied in several different models with a long-range interaction. See Refs. [30, 31] and references therein.

7. Conclusions

There is the compelling evidence that, in muscovite mica, there exists some excitation that propagates extremely long distances, as compared with the lattice constant, even centimeters. Some specimens of muscovite show dark lines which are precipitations or iron oxide. Some of these lines have been shown to be tracks produced by elementary charged particles, like muons and positrons. This proves that, at some sensitive period of its formation, muscovite has had an amazing recording capability of disturbances. Most of the lines are not produced by charged particles but by some kind of excitation, called quodon, propagating in the cation layer along close packed lines. The experiment have shown that this excitation can travel a few millimeters with enough energy to eject an atom at the surface. However, its exact nature is yet not well known.

The models proposed so far have overlooked that the cations have an exclusively repulsive interaction without an equilibrium point. We have proposed a minimal model of repulsive particles. It does not intend to reproduce exactly the extremely complex structure and properties of the mineral, but to explore the peculiarities of a repulsive lattice with respect to the propagation of localized excitations.

We have found that the kinks are easily excited and propagate along the lattice. Basically, any perturbation with sufficient energy produces them and can be modulated to produce any number of them with almost any energy. The relationship between the kink velocity and the amplitude has been obtained, and we have shown that it has good agreement with the numerical results. The kink velocities can be an order of magnitude larger than the speed of sound, and its energy can be of hundreds of eV, even keV.

The study of a more realistic version of this system is under way. The first step will be to add a short-range potential of the type used in ion collisions that will prevent the particles to become too close. The results will be reported elsewhere in due time, but we anticipate that the supersonic kinks with large energies will also appear.

1. D.A. Young, Nature **182**, 375 (1958).
2. E.C.H. Silk and R.S. Barnes, Philos. Mag. **4**, 970 (1959).
3. P.B. Price and R.M. Walker, Nature **196**, 732 (1962).
4. M. Maurette, P. Pellas, and R.M. Walker, Nature **204**, 821 (1964).
5. H.J. Rose and G.A. Jones, Nature **307**, 245 (1984).
6. V.P. Perelygin, Yu.V. Bondar, W. Ensinger, R.L. Fleischer, P. Vater, and S.G. Stetsenko, Nucl. Phys. A, **723**, 410 (2003).
7. S.A. Durrani, Rad. Meas. **34**, 5 (2001).
8. S.A. Durrani, Rad. Meas. **43**, S26 (2008).
9. L.A. Pérez-Maqueda, F. Franco, M.A. Avilés, J. Poyato, and J.L. Pérez-Maqueda, Clays and Clay Miner. **51**, 701 (2003).
10. F.M. Russell, Phys. Lett. B **25**, 298 (1967).
11. F.M. Russell, Nature **216**, 907 (1967).
12. F.M. Russell, Nature **217**, 51 (1967).
13. F.M. Russell, Phys. Lett. A **130**, 489 (1988).
14. F. Russell, Nucl. Tracks. Rad. Meas. **15**, 41 (1988).
15. A.M. Kosevich and A.S. Kovalev, Sov. Phys. JETP **67**, 1793 (1974).
16. A.J. Sievers and S. Takeno, Phys. Rev. Lett. **61**, 970 (1988).
17. K. Kroneberger, M. Schosnig, F.M. Russell, and K.O. Groeneveld, Rad. Meas. **23**, 209 (1994).
18. F.M. Russell and J.C. Eilbeck, Europhys. Lett. **78**, 10004 (2007).
19. J.F.R. Archilla, J. Cuevas, M.D. Alba, M. Naranjo, and J.M. Trillo, J. Phys. Chem. B **110(47)**, 24112 (2006).
20. J.F.R Archilla, J. Cuevas, and F. R. Romero, AIP Conf. Proc. **982(1)**, 788 (2008).
21. V.I. Dubinko, P.A. Selyshchev, and J.F.R. Archilla, Phys. Rev. E **83**, 041124 (2011).

22. Yu.A. Kosevich, R. Khomeriki, and S. Ruffo, Europhys. Lett. **66**, 21 (2004).

23. G. Brudeylins and D. Schmicker, Surf. Sci. **333**, 237 (1995).

24. D.R. Collins, W.G. Stirling, C.R.A. Catlow, and G. Rowbotham, Phys. Chem. Miner. **19**, 520 (1993).

25. N. Wada and W.A. Kamitakahara, Phys. Rev. B **43**, 2391 (1991).

26. S.L. Chaplot and et al. Eur. J. Min. **14**, 291 (2002).

27. Yu.A. Kosevich, Phys. Rev. Lett. **71**, 2058 (1993).

28. B. Sánchez-Rey, G. James, J. Cuevas, and J.F.R. Archilla, Phys. Rev. B **70**, 014301 (2004).

29. J.B. Page, Phys. Rev. B **41**, 7835 (1990).

30. C. Brunhuber, F.G. Mertens, and Y. Gaididei, Eur. Phys. J. B **57**, 57 (2007).

31. C. Brunhuber, F.G. Mertens, and Y.B. Gaididei, Phys. Rev. E **75**, 036615 (2007).

*Дж.Ф.Р. Арчілла, Ю.А. Косевич, Н. Жіменес,
В.Дж. Санчес-Морчілло, Л.М. Гарсіа-Раффі*

РУШІЙНІ ЗБУДЖЕННЯ В КАТІОННИХ ҐРАТКАХ

Р е з ю м е

Розглянуто модель з тотожними частинками, які відштовхують одна одну завдяки кулонівській взаємодії. Чисельно і аналітично досліджено питання про існування і властивості надзвукових кінків, які дуже легко генеруються і проходять великі відстані. Кінкі мають швидкості і енергії в широкому діапазоні. Нас мотивувала особлива характеристика мінералу мусковіт. У складній структурі можна розрізняти треки від частинок, таких як мюони, і більшість треків може бути пояснено в термінах локалізованих збуджень, званих кодонами. Вони рухаються в ґратці катіонів між шарами силікату вздовж напрямків ґратки. Кодони виявлено експериментально в роботі EPL **78**, 1005 (2007).